AD-A064 616 OAKLAND UNIV ROCHESTER MICH SCHOOL OF ENGINEERING F/G 20/11
OPTIMUM HOLE SHAPES IN FINITE PLATES UNDER UNIAXIAL LOAD,(U)
FEB 79 A J DURELLI, K RAJAIAH N00014-76-C-0487
UNCLASSIFIED 50 NL

1 OF 1
AD
A064616

END
DATE
FILMED
4-79
DDC

LEVEL II

OPTIMUM HOLE SHAPES IN FINITE PLATES UNDER UNIAXIAL LOAD

BY

A. J. DURELLI AND K. RAJAIAH

SPONSORED BY

OFFICE OF NAVAL RESEARCH
DEPARTMENT OF THE NAVY
WASHINGTON, D.C. 20025

ON

CONTRACT No. N00014-76-C-0487
O.U. PROJECT No. 31414-24
REPORT No. 50

AND

NATIONAL SCIENCE FOUNDATION
WASHINGTON, D.C. 20550

ON

GRANT No. ENG77-07974
O.U. PROJECT No. 32110-18

SCHOOL OF ENGINEERING
OAKLAND UNIVERSITY
ROCHESTER, MICHIGAN 48063

FEBRUARY 1979

OPTIMUM HOLE SHAPES IN FINITE PLATES UNDER UNIAXIAL LOAD

by

A. J. Durelli and K. Rajaiah

Sponsored by

Office of Naval Research
Department of the Navy
Washington, D.C. 20025

on

Contract No. N00014-76-C-0487
OU Project No. 31414-24
Report No. 50

and

National Science Foundation
Washington, D.C. 20550

on

Grant No. ENG77-07974
OU Project No. 32110-18

School of Engineering
Oakland University
Rochester, Michigan 48063

February 1979

Previous Technical Reports to the Office of Naval Research

1. A. J. Durelli, "Development of Experimental Stress Analysis Methods to Determine Stresses and Strains in Solid Propellant Grains"--June 1962.
Developments in the manufacturing of grain-propellant models are reported. Two methods are given: a) cementing routed layers and b) casting.

2. A. J. Durelli and V. J. Parks, "New Method to Determine Restrained Shrinkage Stresses in Propellant Grain Models"--October 1962.
The birefringence exhibited in the curing process of a partially restrained polyurethane rubber is used to determine the stress associated with restrained shrinkage in models of solid propellant grains partially bonded to the case.

3. A. J. Durelli, "Recent Advances in the Application of Photoelasticity in the Missile Industry"--October 1962.
Two- and three-dimensional photoelastic analysis of grains loaded by pressure and by temperature are presented. Some applications to the optimization of fillet contours and to the redesign of case joints are also included.

4. A. J. Durelli and V. J. Parks, "Experimental Solution of Some Mixed Boundary Value Problems"--April 1964.
Means of applying known displacements and known stresses to the boundaries of models used in experimental stress analysis are given. The application of some of these methods to the analysis of stresses in the field of solid propellant grains is illustrated. The presence of the "pinching effect" is discussed.

5. A. J. Durelli, "Brief Review of the State of the Art and Expected Advance in Experimental Stress and Strain Analysis of Solid Propellant Grains"--April 1964.
A brief review is made of the state of the experimental stress and strain analysis of solid propellant grains. A discussion of the prospects for the next fifteen years is added.

6. A. J. Durelli, "Experimental Strain and Stress Analysis of Solid Propellant Rocket Motors"--March 1965.
A review is made of the experimental methods used to strain-analyze solid propellant rocket motor shells and grains when subjected to different loading conditions. Methods directed at the determination of strains in actual rockets are included.

7. L. Ferrer, V. J. Parks and A. J. Durelli, "An Experimental Method to Analyze Gravitational Stresses in Two-Dimensional Problems"--October 1965.
Photoelasticity and moiré methods are used to solve two-dimensional problems in which gravity-stresses are present.

8. A. J. Durelli, V. J. Parks and C. J. del Rio, "Stresses in a Square Slab Bonded on One Face to a Rigid Plate and Shrunk"--November 1965.
A square epoxy slab was bonded to a rigid plate on one of its faces in the process of curing. In the same process the photoelastic effects associated with a state of restrained shrinkage were "frozen-in." Three-dimensional photoelasticity was used in the analysis.

9. A. J. Durelli, V. J. Parks and C. J. del Rio, "Experimental Determination of Stresses and Displacements in Thick-Wall Cylinders of Complicated Shape"--April 1966.
Photoelasticity and moiré are used to analyze a three-dimensional rocket shape with a star shaped core subjected to internal pressure.

10. V. J. Parks, A. J. Durelli and L. Ferrer, "Gravitational Stresses Determined Using Immersion Techniques"--July 1966.
The methods presented in Technical Report No. 7 above are extended to three-dimensions. Immersion is used to increase response.

11. A. J. Durelli and V. J. Parks. "Experimental Stress Analysis of Loaded Boundaries in Two-Dimensional Second Boundary Value Problems"--February 1967.
The pinching effect that occurs in two-dimensional bonding problems, noted in Reports 2 and 4 above, is analyzed in some detail.

12. A. J. Durelli, V. J. Parks, H. C. Feng and F. Chiang, "Strains and Stresses in Matrices with Inserts,"-- May 1967.
Stresses and strains along the interfaces, and near the fiber ends, for different fiber end configurations, are studied in detail.

13. A. J. Durelli, V. J. Parks and S. Uribe, "Optimization of a Slot End Configuration in a Finite Plate Subjected to Uniformly Distributed Load,"--June 1967.
Two-dimensional photoelasticity was used to study various elliptical ends to a slot, and determine which would give the lowest stress concentration for a load normal to the slot length.

14. A. J. Durelli, V. J. Parks and Han-Chow Lee, "Stresses in a Split Cylinder Bonded to a Case and Subjected to Restrained Shrinkage,"--January 1968.
A three-dimensional photoelastic study that describes a method and shows results for the stresses on the free boundaries and at the bonded interface of a solid propellant rocket.

15. A. J. Durelli, "Experimental Stress Analysis Activities in Selected European Laboratories"--August 1968.
This report has been written following a trip conducted by the author through several European countries. A list is given of many of the laboratories doing important experimental stress analysis work and of the people interested in this kind of work. An attempt has been made to abstract the main characteristics of the methods used in some of the countries visited.

16. V. J. Parks, A. J. Durelli and L. Ferrer, "Constant Acceleration Stresses in a Composite Body"--October 1968.
Use of the immersion analogy to determine gravitational stresses in two-dimensional bodies made of materials with different properties.

17. A. J. Durelli, J. A. Clark and A. Kochev, "Experimental Analysis of High Frequency Stress Waves in a Ring"--October 1968.
A method for the complete experimental determination of dynamic stress distributions in a ring is demonstrated. Photoelastic data is supplemented by measurements with a capacitance gage used as a dynamic lateral extensometer.

18. J. A. Clark and A. J. Durelli, "A Modified Method of Holographic Interferometry for Static and Dynamic Photoelasticity"--April 1968.
A simplified absolute retardation approach to photoelastic analysis is described. Dynamic isopachics are presented.

19. J. A. Clark and A. J. Durelli, "Photoelastic Analysis of Flexural Waves in a Bar"--May 1969.
A complete direct, full-field optical determination of dynamic stress distribution is illustrated. The method is applied to the study of flexural waves propagating in a urethane rubber bar. Results are compared with approximate theories of flexural waves.

20. J. A. Clark and A. J. Durelli, "Optical Analysis of Vibrations in Continuous Media"--June 1969.
Optical methods of vibration analysis are described which are independent of assumptions associated with theories of wave propagation. Methods are illustrated with studies of transverse waves in prestressed bars, snap loading of bars and motion of a fluid surrounding a vibrating bar.

21. V. J. Parks, A. J. Durelli, K. Chandrashekhara and T. L. Chen, "Stress Distribution Around a Circular Bar, with Flat and Spherical Ends, Embedded in a Matrix in a Triaxial Stress Field"--July 1969.
A Three-dimensional photoelastic method to determine stresses in composite materials is applied to this basic shape. The analyses of models with different loads are combined to obtain stresses for the triaxial cases.

22. A. J. Durelli, V. J. Parks and L. Ferrer, "Stresses in Solid and Hollow Spheres Subjected to Gravity or to Normal Surface Tractions"--October 1969.
The method described in Report No. 10 above is applied to two specific problems. An approach is suggested to extend the solutions to a class of surface traction problems.

23. J. A. Clark and A. J. Durelli, "Separation of Additive and Subtractive Moiré Patterns"--December 1969.
A spatial filtering technique for adding and subtracting images of several gratings is described and employed to determine the whole field of Cartesian shears and rigid rotations.

24. R. J. Sanford and A. J. Durelli, "Interpretation of Fringes in Stress-Holo-Interferometry"--July 1970.
Errors associated with interpreting stress-holo-interferometry patterns as the superposition of isopachics (with half order fringe shifts) and isochromatics are analyzed theoretically and illustrated with computer generated holographic interference patterns.

25. J. A. Clark, A. J. Durelli and P. A. Laura, "On the Effect of Initial Stress on the Propagation of Flexural Waves in Elastic Rectangular Bars"--December 1970.
Experimental analysis of the propagation of flexural waves in prismatic, elastic bars with and without prestressing. The effects of prestressing by axial tension, axial compression and pure bending are illustrated.

26. A. J. Durelli and J. A. Clark, "Experimental Analysis of Stresses in a Buoy-Cable System Using a Birefringent Fluid"--February 1971.
An extension of the method of photoviscous analysis is presented which permits quantitative studies of strains associated with steady state vibrations of immersed structures. The method is applied in an investigation of one form of behavior of buoy-cable systems loaded by the action of surface waves.

27. A. J. Durelli and T. L. Chen, "Displacements and Finite-Strain Fields in a Sphere Subjected to Large Deformations"--February 1972.
Displacements and strains (ranging from 0.001 to 0.50) are determined in a polyurethane sphere subjected to several levels of diametral compression. A 500 lines-per-inch grating was embedded in a meridian plane of the sphere and moiré effect produced with a non-deformed master. The maximum applied vertical displacement reduced the diameter of the sphere by 27 per cent.

28. A. J. Durelli and S. Machida, "Stresses and Strain in a Disk with Variable Modulus of Elasticity"--March 1972
A transparent material with variable modulus of elasticity has been manufactured that exhibits good photoelastic properties and can also be strain analyzed by moiré. The results obtained suggests that the stress distribution in the disk of variable E is practically the same as the stress distribution in the homogeneous disk. It also indicates that the strain fields in both cases are very different, but that it is possible, approximately, to obtain the stress field from the strain field using the value of E at every point, and Hooke's law.

29. A. J. Durelli and J. Buitrago, "State of Stress and Strain in a Rectangular Belt Pulled Over a Cylindrical Pulley"--June 1972.
Two- and three-dimensional photoelasticity as well as electrical strain gages, dial gages and micrometers are used to determine the stress distribution in a belt-pulley system. Contact and tangential stress for various contact angles and friction coefficients are given.

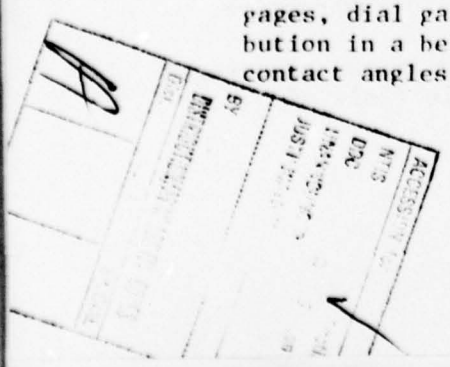

30. T. L. Chen and A. J. Durelli, "Stress Field in a Sphere Subjected to Large Deformations"--June 1972.
Strain fields obtained in a sphere subjected to large diametral compressions from a previous paper were converted into stress fields using two approaches. First, the concept of strain-energy function for an isotropic elastic body was used. Then the stress field was determined with the Hookean type natural stress-natural strain relation. The results so obtained were also compared.

31. A. J. Durelli, V. J. Parks and H. M. Hasseem, "Helices Under Load"--July 1973.
Previous solutions for the case of close coiled helical springs and for helices made of thin bars are extended. The complete solution is presented in graphs for the use of designers. The theoretical development is correlated with experiments.

32. T. L. Chen and A. J. Durelli, "Displacements and Finite Strain Fields in a Hollow Sphere Subjected to Large Elastic Deformations"--September 1973.
The same methods described in No. 27, were applied to a hollow sphere with an inner diameter one half the outer diameter. The hollow sphere was loaded up to a strain of 30 per cent on the meridian plane and a reduction of the diameter by 20 per cent.

33. A. J. Durelli, H. H. Hasseem and V. J. Parks, "New Experimental Method in Three-Dimensional Elastostatics"--December 1973.
A new material is reported which is unique among three-dimensional stress-freezing materials, in that, in its heated (or rubbery) state it has a Poisson's ratio which is appreciably lower than 0.5. For a loaded model, made of this material, the unique property allows the direct determination of stresses from strain measurements taken at interior points in the model.

34. J. Wolak and V. J. Parks, "Evaluation of Large Strains in Industrial Applications"--April 1974.
It was shown that Mohr's circle permits the transformation of strain from one axis of reference to another, irrespective of the magnitude of the strain, and leads to the evaluation of the principal strain components from the measurement of direct strain in three directions.

35. A. J. Durelli, "Experimental Stress Analysis Activities in Selected European Laboratories"--April 1975.
Continuation of Report No. 15 after a visit to Belgium, Holland, Germany, France, Turkey, England and Scotland.

36. A. J. Durelli, V. J. Parks and J. O. Bühler-Vidal, "Linear and Non-linear Elastic and Plastic Strains in a Plate with a Big Hole Loaded Axially in its Plane"--July 1975.
Strain analysis of the ligament of a plate with a big hole indicates that both geometric and material non-linearity may take place. The strain concentration factor was found to vary from 1 to 2 depending on the level of deformation.

37. A. J. Durelli, V. Pavlin, J. O. Bühler-Vidal and G. Ome, "Elastostatics of a Cubic Box Subjected to Concentrated Loads"--August 1975.
Analysis of experimental strain, stress and deflection of a cubic box subjected to concentrated loads applied at the center of two opposite faces. The ratio between the inside span and the wall thickness was varied between approximately 5 and 121.

38. A. J. Durelli, V. J. Parks and J. O. Bühler-Vidal, "Elastostatics of Cubic Boxes Subjected to Pressure"--March 1976.
Experimental analysis of strain, stress and deflections in a cubic box subjected to either internal or external pressure. Inside span-to-wall thickness ratio varied from 5 to 14.

39. Y. Y. Hung, J. D. Hovanesian and A. J. Durelli, "New Optical Method to Determine Vibration-Induced Strains with Variable Sensitivity After Recording"--November 1976.
A steady state vibrating object is illuminated with coherent light and its image slightly misfocused. The resulting specklegram is "time-integrated" as when Fourier filtered gives derivatives of the vibrational amplitude.

40. Y. Y. Hung, C. Y. Liang, J. D. Hovanesian and A. J. Durelli, "Cyclic Stress Studies by Time-Averaged Photoelasticity"--November 1976.
"Time-averaged isochromatics" are formed when the photographic film is exposed for more than one period. Fringes represent amplitudes of the oscillating stress according to the zeroth order Bessel function.

41. Y. Y. Hung, C. Y. Liang, J. D. Hovanesian and A. J. Durelli, "Time-Averaged Shadow Moiré Method for Studying Vibrations"--November 1976.
Time-averaged shadow moiré permits the determination of the amplitude distribution of the deflection of a steady vibrating plate.

42. J. Buitrago and A. J. Durelli, "On the Interpretation of Shadow-Moiré Fringes"--April 1977.
Possible rotations and translations of the grating are considered in a general expression to interpret shadow-moiré fringes and on the sensitivity of the method. Application to an inverted perforated tube.

43. J. der Hovanesian, "18th Polish Solid Mechanics Conference." Published in European Scientific Notes of the Office of Naval Research, in London, England, Dec. 31, 1976.
Comments on the planning and organization of, and scientific content of paper presented at the 18th Polish Solid Mechanics Conference held in Wisla-Jawornik from September 7-14, 1976.

44. A. J. Durelli, "The Difficult Choice,"--May 1977.
The advantages and limitations of methods available for the analyses of displacements, strain, and stresses are considered. Comments are made on several theoretical approaches, in particular approximate methods, and attention is concentrated on experimental methods: photo-elasticity, moiré, brittle and photoelastic coatings, gages, grids, holography and speckle to solve two- and three-dimensional problems in elasticity, plasticity, dynamics and anisotropy.

45. C. Y. Liang, Y. Y. Hung, A. J. Durelli and J. D. Hovanesian, "Direct Determination of Flexural Strains in Plates Using Projected Gratings,"--June 1977.
The method requires the rotation of one photograph of the deformed grating over a copy of itself. The moiré produced yields strains by optical double differentiation of deflections. Applied to projected gratings the idea permits the study of plates subjected to much larger deflections than the ones that can be studied with holograms.

46. A. J. Durelli, K. Brown and P. Yee, "Optimization of Geometric Discontinuities in Stress Fields"--March 1978.
The concept of "coefficient of efficiency" is introduced to evaluate the degree of optimization. An ideal design of the inside boundary of a tube subjected to diametral compression is developed which decreases its maximum stress by 25%, at the time it also decreases its weight by 10%. The efficiency coefficient is increased from 0.59 to 0.95. Tests with a brittle material show an increase in strength of 20%. An ideal design of the boundary of the hole in a plate subjected to axial load reduces the maximum stresses by 26% and increases the coefficient of efficiency from 0.54 to 0.90.

47. J. D. Hovanesian, Y. Y. Hung and A. J. Durelli, "New Optical Method to Determine Vibration-Induced Strains With Variable Sensitivity After Recording"--May 1978.
A steady-state vibrating object is illuminated with coherent light and its image is slightly misfocused in the film plane of a camera. The resulting processed film is called a "time-integrated specklegram." When the specklegram is Fourier filtered, it exhibits fringes depicting derivatives of the vibrational amplitude. The direction of the spatial derivative, as well as the fringe sensitivity may be easily and continuously varied during the Fourier filtering process. This new method is also much less demanding than holographic interferometry with respect to vibration isolation, optical set-up time, illuminating source coherence, required film resolution. etc.

48. Y. Y. Hung and A. J. Durelli, "Simultaneous Determination of Three Strain Components in Speckle Interferometry Using a Multiple Image Shearing Camera,"--September 1978
This paper describes a multiple image-shearing camera. Incorporating coherent light illumination, the camera serves as a multiple shearing speckle interferometer which measures the derivatives of surface displacements with respect to three directions simultaneously. The application of the camera to the study of flexural strains in bent plates is shown, and the determination of the complete state of two-dimensional strains is also considered. The multiple image-shearing camera uses an interference phenomena, but is less demanding than holographic interferometry with respect to vibration isolation and the coherence of the light source. It is superior to other speckle techniques in that the obtained fringes are of much better quality.

49. This paper deals with the optimization of the shape of the corners and sides of a square hole, located in a large plate and subjected to in-plane loads. Appreciable disagreement has been found between the results obtained previously by other investigators. Using an optimization technique, the authors have developed a quasi square shape which introduces a stress concentration of only 2.54 in a uniaxial field, the comparable value for the circular hole being 3. The efficiency factor of the proposed optimum shape is 0.90 whereas the one of the best shape developed previously was 0.71. The shape also is developed that minimizes the stress concentration in the case of biaxial loading when the ratio of biaxiality is 1:-1.

OPTIMUM HOLE SHAPES IN FINITE PLATES UNDER UNIAXIAL LOAD

by

A. J. Durelli and K. Rajaiah

Abstract

This paper presents optimized hole shapes in plates of finite width subjected to uniaxial load for a large range of hole to plate widths (D/W) ratios. The stress concentration factor for the optimized holes decreased by as much as 44% when compared to circular holes. Simultaneously, the area covered by the optimized hole increased by as much as 26% compared to the circular hole. Coefficients of efficiency between 0.91 and 0.96 are achieved. The geometries of the optimized holes for the D/W ratios considered are presented in a form suitable for use by designers. It is also suggested that the developed geometries may be applicable to cases of rectangular holes and to the tip of a crack. This information may be of interest in fracture mechanics.

Introduction

Optimization of hole shapes in stress fields is an important problem in engineering design. Surprisingly, the problem has attracted very limited attention. Heywood[1] was one of the first investigators to attempt the optimization of hole shapes and, based on general considerations, he predicted that a barrel-shaped hole with the bulging sides having a radius of curvature equal to the hole width D would be an optimum shape for an infinite plate under uniaxial tension. Ross[2] conducted photoelastic experiments on Heywood's "ideal shape" hole and estimated the stress concentration factor (s.c.f.) to be 3.25.

Durelli, Dally and Riley[3], and more recently, Durelli, Brown and Yee[4] presented a practical way of arriving at optimum hole shapes from simple photoelastic tests by removal of material from low stress regions around the hole and making an isochromatic fringe coincide with the boundary. Following this approach, Durelli and Rajaiah[5] arrived at a quasi-square hole with a s.c.f. value of only 2.54 as optimum shape for a wide plate under uniaxial load, and a double-barrel hole with a s.c.f. value of only 3.6 as optimum shape for a wide plate under pure shear, the corresponding values for the circular hole being 3 and 4 respectively. In the present paper, work on the optimization of hole shapes in finite plates subjected to uniaxial load is presented.

Constraints of the Problem

For the optimization process, the following constraints were stipulated:

a) the boundary of the hole has to lie inbetween the circle of diameter D and the square of side D. and

b) the allowable maximum stress for compression is about three times the allowable maximum stress for tension.

Method

As already mentioned, the optimization process involves removal of material from low stress regions around the hole by careful hand filing till an isochromatic fringe coincides with the boundary in the tensile and compressive regions respectively. The constraints of the problem dictate the amount of material that may be removed.

It was proposed in an earlier paper[4] that the degree of optimization be evaluated quantitatively by a coefficient of efficiency

$$k_{eff} = \frac{1}{S_2 - S_0} \left\{ \frac{\int_{S_0}^{S_1} \sigma_t^+ ds}{\sigma_{all}^+} + \frac{\int_{S_1}^{S_2} \sigma_t^- ds}{\sigma_{all}^-} \right\}$$

where σ_{all} represents the maximum allowable stress (the positive and negative superscripts referring to tensile and compressive stresses, respectively), S_0 and S_1 are the limiting points of the segment of boundary subjected to tensile stresses and S_1 and S_2 are the limiting points of the segment of boundary with compressive stresses.

The coefficient of efficiency k_{eff} shows how efficiently the material at the hole boundary has been utilized for the given field. k_{eff} equal to one would mean that the stress levels are constant both on the tensile and compressive regions around the hole. The closer k_{eff} is to unity, the more efficient the design is. In other words, a hole with a k_{eff} of 0.95 has a higher degree of optimization than a hole with a $k_{eff} = 0.90$. Further, as one moves from a k_{eff} value of about say 0.80 to say 0.95, the s.c.f. comes down in both the tensile and compressive regions.

The same criterion has been used in the present work to evaluate the optimized hole shapes.

Experimental Details

Experiments were conducted with 0.23 in (5.8mm) thick Homalite-100 plates (fringe constant of 133.2 lb/in-fr (23.3 kN/m-fr)). The hole width was chosen as 1.5 in (38.1 mm) for the smaller D/W ratios while it was maintained at 3.0 in (76.2 mm) for the larger D/W ratios. Optimization was carried out for D/W = 0.140, 0.377, 0.518, 0.775 and 0.837, with the models subjected to uniaxial tension. For small ratios, the absolute size of the hole had to be kept small for practical considerations of the loading frame, while for large ratios, larger hole sizes could be chosen. Invariably, the use of larger hole sizes increases the ease with which optimization can be carried out especially at the corners, and improves the precision of the determinations. To improve the precision further, in particular at the corner zones, a binocular magnifier with a set of polarizer and quarter wave plates attached to each of its lenses was used during the filing process.

Results

The isochromatic patterns for two typical hole shapes are shown in Figs. 1 and 2. The stress distributions around the optimized holes for the D/W ratios considered are presented in Fig. 3. The same figure also includes the stress distribution around circular holes in several plates of finite width. The s.c.f. for the tensile and compressive regions of the optimized holes for different D/W ratios are plotted in Fig. 4. Information for circular holes[6] is also included in this figure.

The empirically developed optimum hole geometries have been fitted with a combination of circles of different diameters and common tangents at the points of intersection. The hole geometries for the different D/W

ratios are shown in Figs. 5 to 9.

The information given in Figs. 5 to 9 have been consolidated in Fig. 10 and the different radii of curvature for the hole edges for the range of D/W ratios considered are presented in graphical form. This information should be useful to designers.

Optimization of Rectangular Holes

It may be recalled that the optimum shapes have been developed with one of the constraints stating that the hole should lie inbetween a square of side D and a circle of diameter D. The hole shapes developed suggest that, for D/W ratios larger than about 0.6, since the longitudinal sides remain straight and so do the fringes, the same shapes developed for the quasi-square hole can be expected to remain optimum for rectangular holes (sides a x b) with a/b ratios larger than about 0.4 (Fig. 11a). Similarly for a/W ratios smaller than about 0.4, the quasi-square shape could be used when the sides of the rectangle are larger than about 0.9 (Fig. 11b).

Optimum Shape of a Tip of a Crack

Rice[9] in his analysis of the strain concentration at smooth-ended notch tips, raises the question of the optimum shape of the tip of a crack. Following the reasoning in the previous paragraph, it is also believed that the geometry outlined in Fig. (11b), for small a/W, may on first approximization give the desired optimum shape at the tip of the crack.

Economy of Weight

The optimum shapes developed here have lead to significant reduction in weight as compared to the circular holes. The percentage increase in the area of the optimized hole as compared to the circular hole has been

plotted in Fig. 4 for the different optimum shapes. The increase is about 16% for D/W = 0.14 while it goes up to about 26% for D/W = 0.64. For D/W larger than 0.64, there is a reduction in the gain, the value reaching 18% for D/W = 0.837. It is anticipated that this trend of reduced gain will continue till D/W $\rightarrow$ 1, since the transverse edge will tend to be a near circular edge.

Discussion

The isochromatic patterns in Figs. 1 and 2 and the stress distributions given in Fig. 3 show that the newly developed hole shapes are optimum with the stresses remaining uniform along large portions of the tensile as well as compressive segments of the edge. It is also seen from Figs. 3 and 4 that, as compared to the circular holes[6], the optimum shapes have resulted in significant reduction of s.c.f., the reduction ranging from 16% for D/W = 0.14 to about 44% for D/W = 0.837. Fig. 4 also includes information given in an earlier paper[4] for D/W = 0.6. It is seen that the present datum is a further refinement over the earlier value wherein k_{eff} = 0.90. The coefficient of efficiency k_{eff} has been achieved in the range 0.91 to 0.96, the lower values being for lower D/W ratios, as shown in Fig. 4.

It is known[6],[7] that, for the circular hole, the limiting value of s.c.f. as D/W $\rightarrow$ 1 is about 2.0. In the present case of optimized holes, this limit would appear to be about 1.0, as seen from Fig. 4.

It is important to study the shape of the optimized holes in Figs. 5 to 9 as the D/W ratio increases. For D/W ratios smaller than about 0.56, the holes are barrel-shaped with the longitudinal edges curved and the transverse edges remaining straight. As the D/W ratio increases towards 0.56, the radius of curvature of the bulging sides also increases. In the range 0.56 < D/W < 0.70, both the longitudinal and the transverse sides

remain straight with curved corners. This would mean that, in this range of D/W, a square hole with rounded corners itself is an optimum shape with the proper choice of corner radius. The information in Fig. 10 confirms this.

As the hole size increases further (D/W > 0.70), interesting things tend to develop. While the longitudinal edges continue to remain straight, the transverse edges start bulging out. The corners need special attention with inflection points appearing along the transverse edges. It would appear that as D/W ratio approaches unity, the transverse edge would tend to become a circular edge with a radius of D/2. Some experimental results of Flynn[7] on circular holes confirm this anticipation.

Another point of interest in Figs. 5-9 is the corner of the hole. It is well accepted that in structural discontinuities any reentrant corner with a very small radius is a potential source of stress concentration and is to be avoided. However, in the present case of optimized holes, the corner regions happen to be low stress areas with zero stress occuring at the corner. Hence, ideally one can have a very sharp reentrant corner without introducing a stress concentration. In other words, the ideal optimized hole with $k_{eff} = 1$ appears to need a sharp corner!

Conclusion

Optimized hole shapes in finite plates subjected to uniaxial load have been presented for a range of D/W ratios. It has been shown that, as compared to circular holes, the optimized holes lead to significant reduction in s.c.f. together with significant increase in the area covered by the hole. Thus a substantial increase in strength/weight ratio is achieved. The geometries of the optimized holes are presented in a form suitable for use by designers. It is also suggested that the developed geometries may be applicable to cases of rectangular holes.

Acknowledgments

The research program from which this paper was developed was supported by the National Science Foundation (Grant ENG-76-07974) and the Office of Naval Research (Contract No. N00014-76-C-0487). The authors are grateful to C. C. Astill of NSF and N. Perrone and N. Basdekas of ONR for their support. The manuscript reproduction has been prepared by P. Baxter and some of the experimental work has been conducted by R. Scott and R. Scicluna.

References

1. Heywood R. B., "Designing by Photoelasticity", Chapman and Hall, 1958.

2. Poss D. S., "Assessing Stress Concentration Factors", Engg. Mat. Design, Vol. 7, pp. 394-398, 1964.

3. Durelli A. J., Dally J. W. and Riley W. F., "Stress and Strength Studies on Turbine Blade Attachments." Proc. S.E.S.A., Vol. XVI, No. 1, pp. 171-182, Dec. 1958.

4. Durelli A. J., Brown K. and Yee P., "Optimization of Geometric Discontinuities in Stress Fields", Exp. Mech., Vol. 18, pp. 303-308, 1978.

5. Durelli A. J. and Rajaiah K., "Quasi-Square Hole with Optimum Shape Subjected to Uniaxial Loading", Oakland University ONR Report No. 49, January 1979.

6. Durelli A. J., Phillips E. A. and Tsao C. H., "Introduction to the Theoretical and Experimental Analysis of Stress and Strain", McGraw Hill, p. 217, 1958.

7. Flynn P. D., "Stress Concentrations in Tensile Strips with Large Circular Holes", Exp. Mech., Vol. 15, pp. 386-388, 1975.

8. Coker E. G. and Filon L. N. G., "A Treatise on Photoelasticity", Cambridge University Press, p. 486, 1931.

9. Rice J. R., "A Path Independent Integral and the Approximate Analysis of Strain Concentration by Notches and Cracks, J. Appl. Mech., Vol. 35, pp. 379-386, 1968.

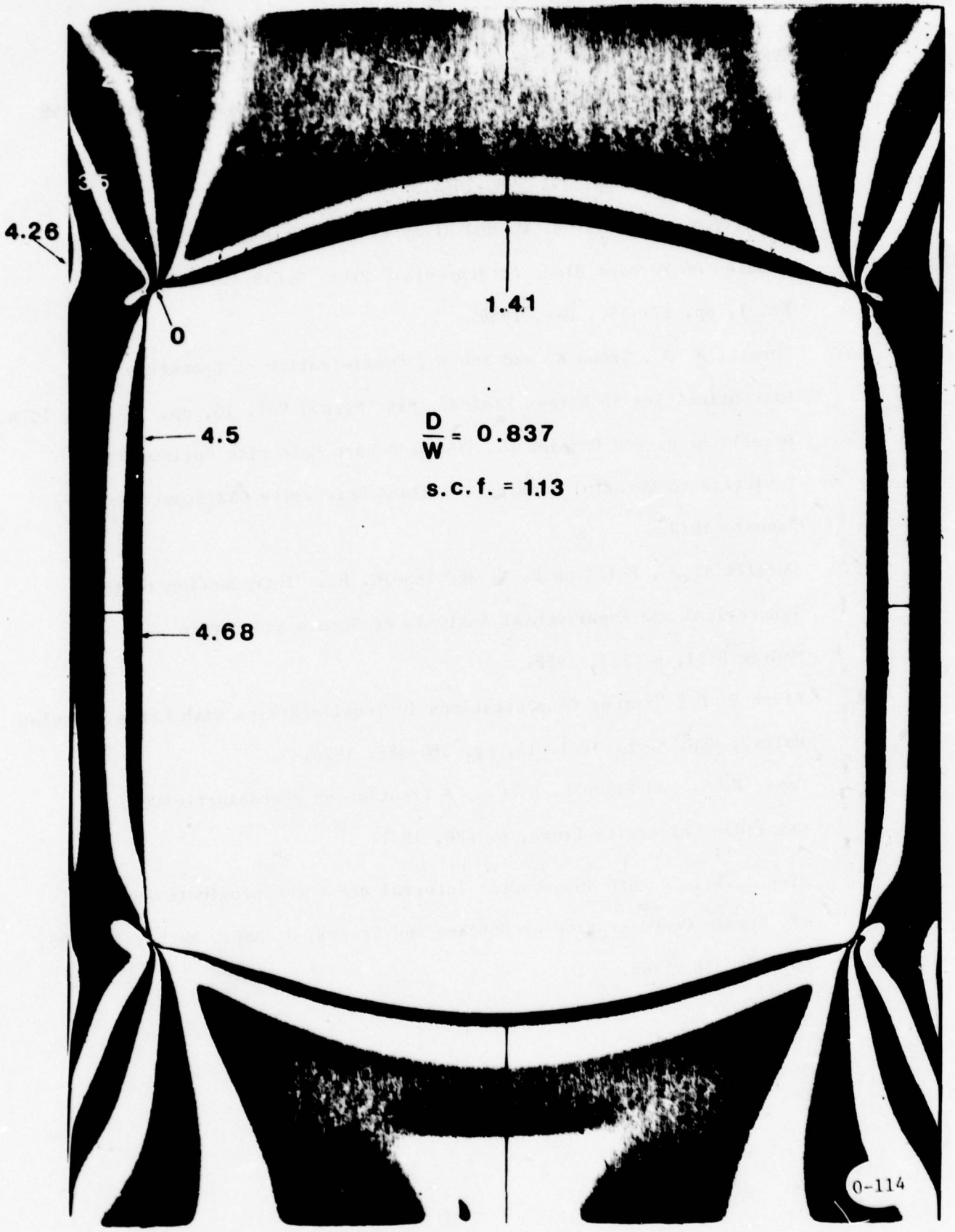

FIG. 1 OPTIMUM SHAPE OF A HOLE IN A FINITE PLATE SUBJECTED TO AXIAL LOADING (D/W = 0.837)

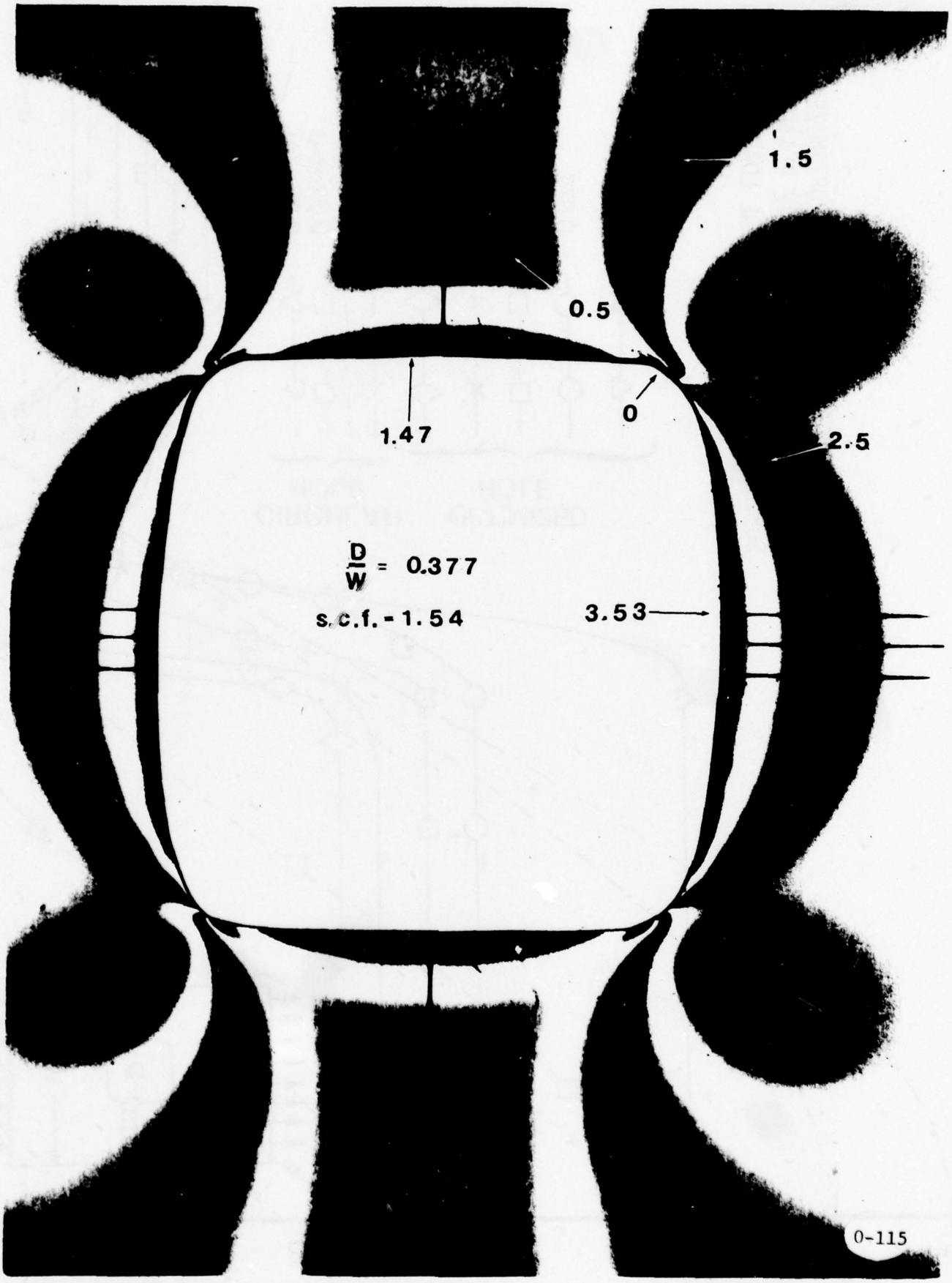

FIG. 2 OPTIMUM SHAPE OF A HOLE IN A PLATE SUBJECTED TO AXIAL LOADING (D/W = 0.377)

FIG. 3 STRESS DISTRIBUTION AROUND OPTIMIZED AND CIRCULAR HOLES IN FINITE PLATES SUBJECTED TO IN-PLANE AXIAL LOADING

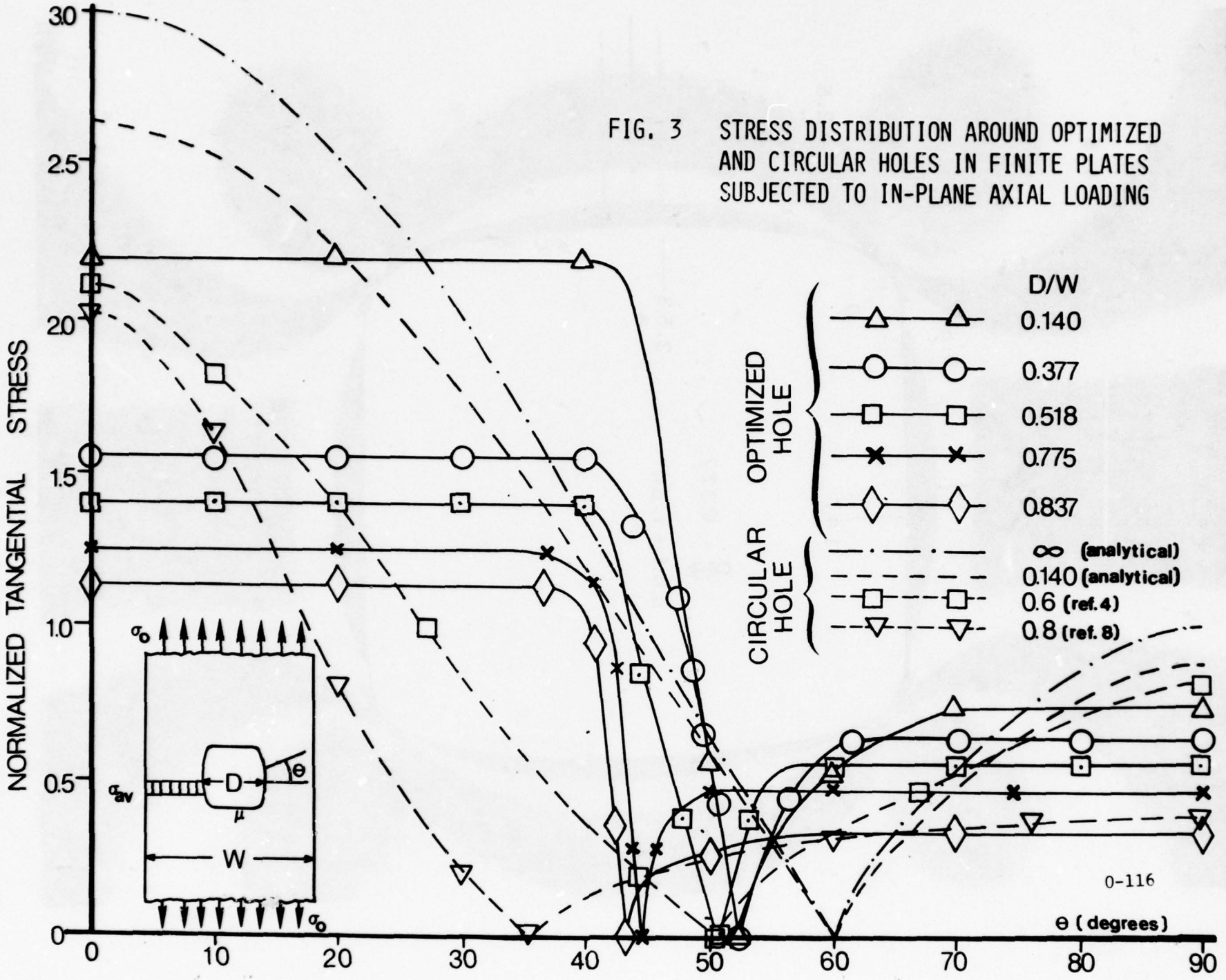

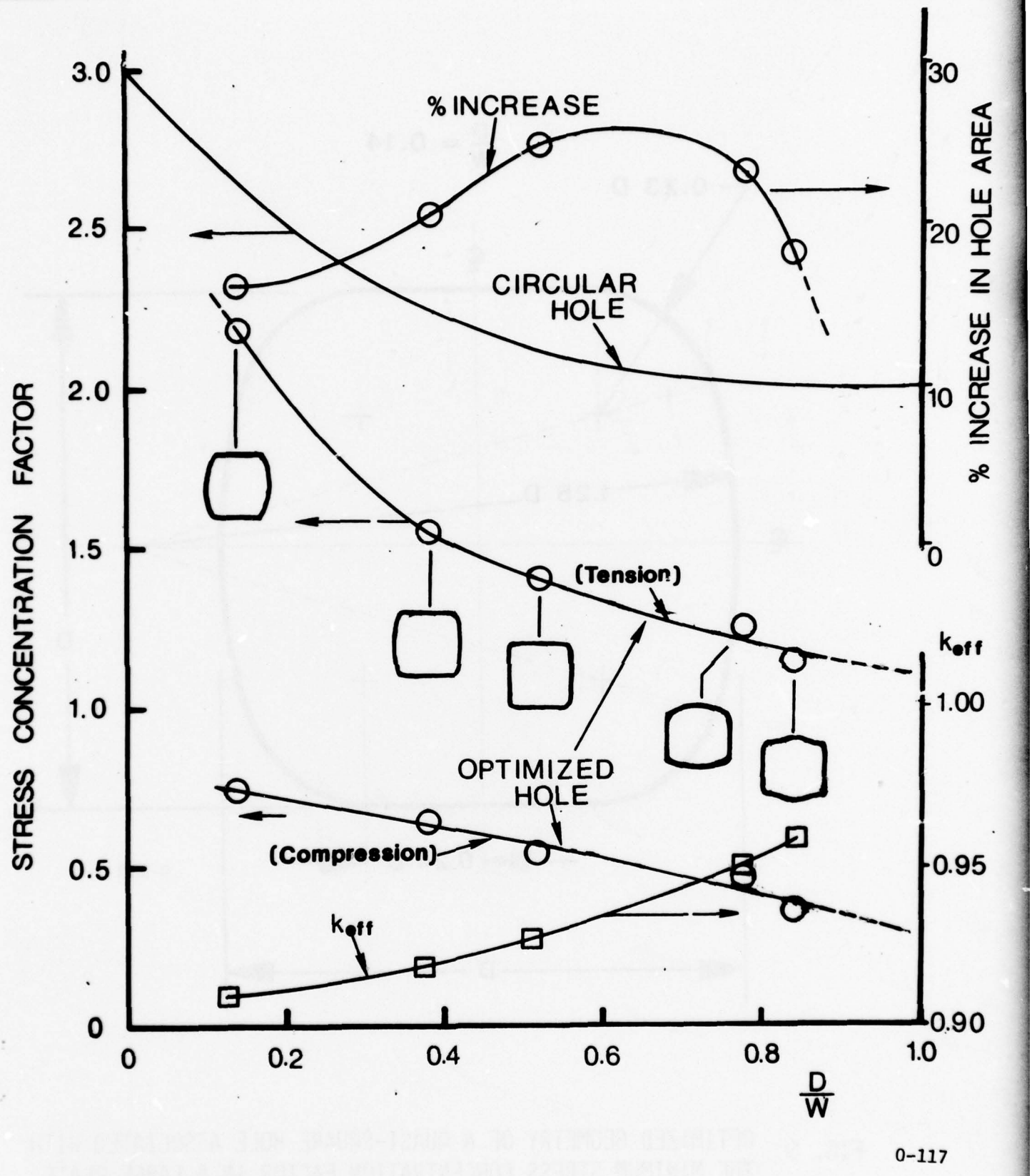

FIG. 4 STRESS CONCENTRATION FACTORS FOR OPTIMIZED HOLES IN FINITE PLATES SUBJECTED TO IN-PLANE AXIAL LOADING

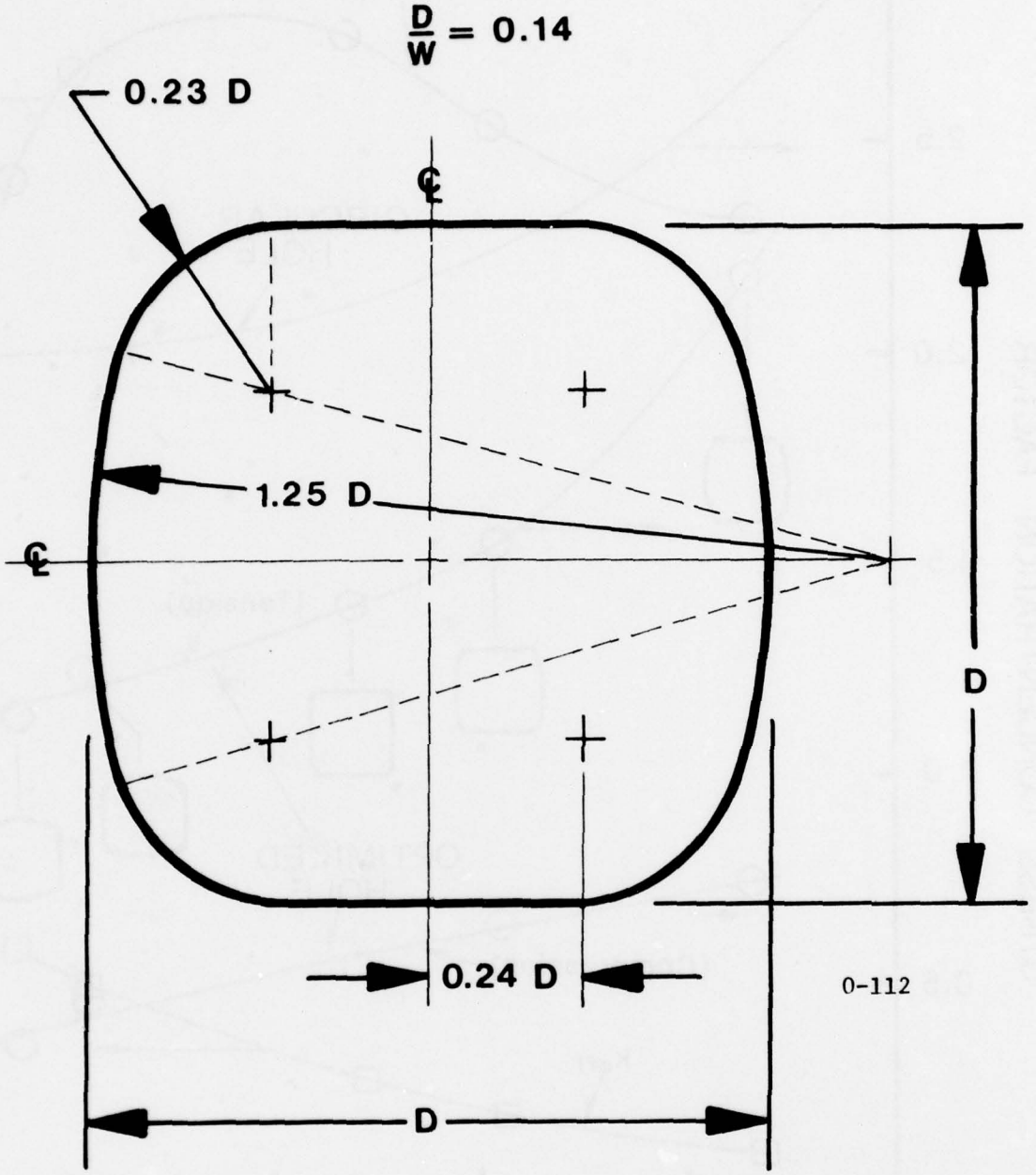

FIG. 5 OPTIMIZED GEOMETRY OF A QUASI-SQUARE HOLE ASSOCIATED WITH THE MINIMUM STRESS CONCENTRATION FACTOR IN A LARGE PLATE SUBJECTED TO UNIAXIAL LOADING

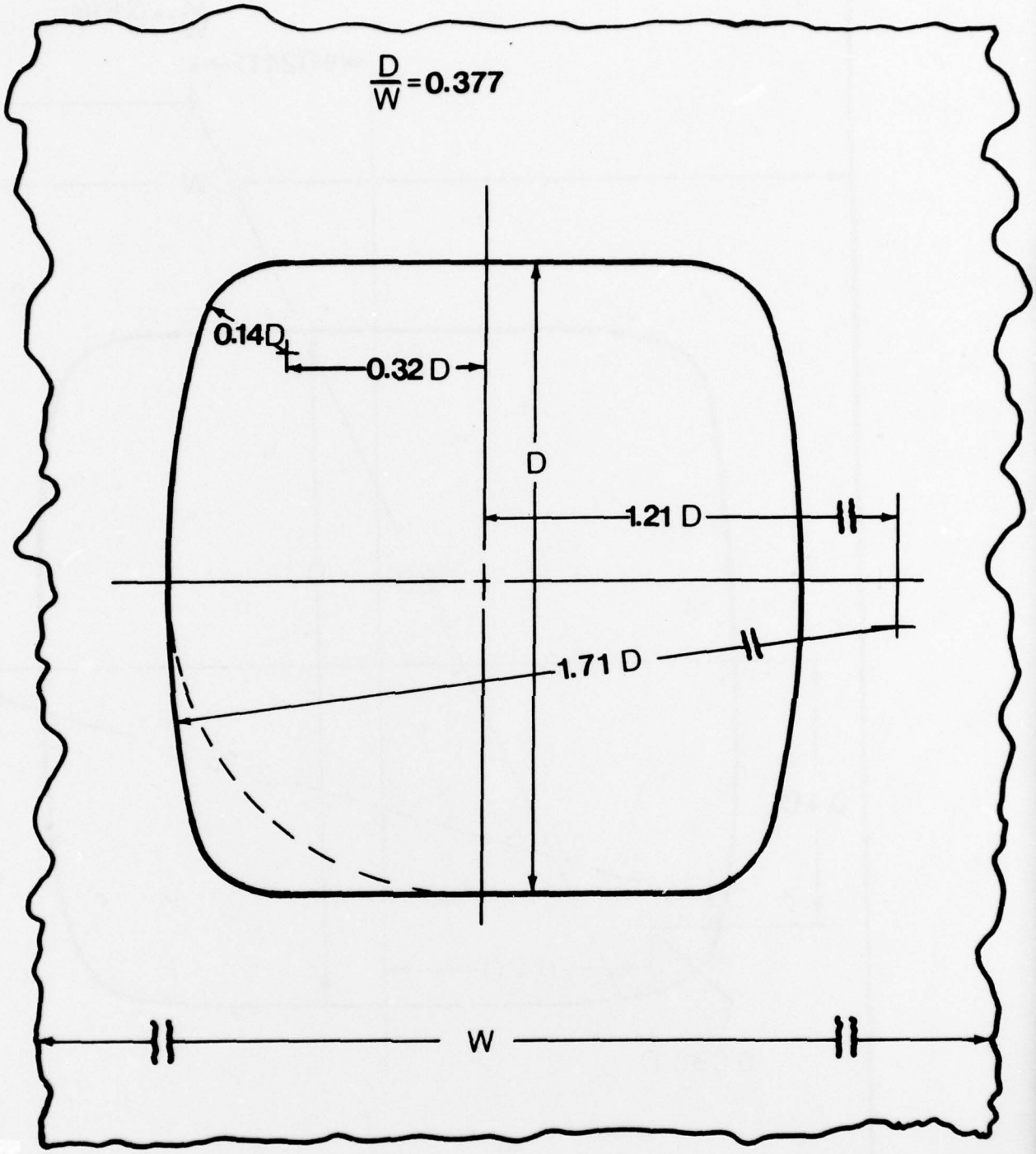

FIG. 6 OPTIMIZED GEOMETRY OF A QUASI-SQUARE HOLE IN FINITE PLATE (D/W = 0.377) SUBJECTED TO IN-PLANE AXIAL LOADING

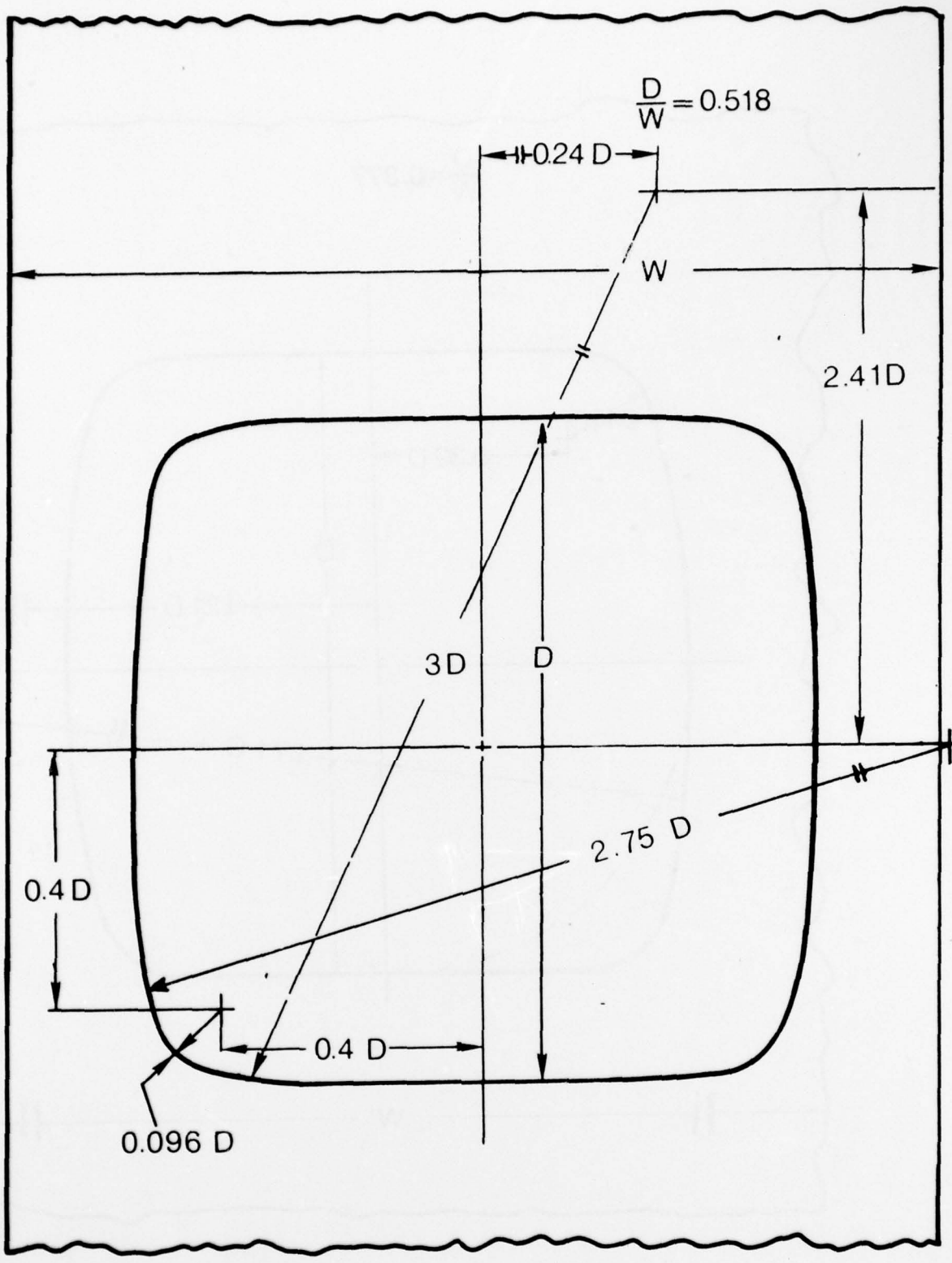

FIG. 7 OPTIMUM GEOMETRY OF A QUASI-SQUARE HOLE IN A FINITE-PLATE (D/W = 0.518) SUBJECTED TO IN-PLANE AXIAL LOADING

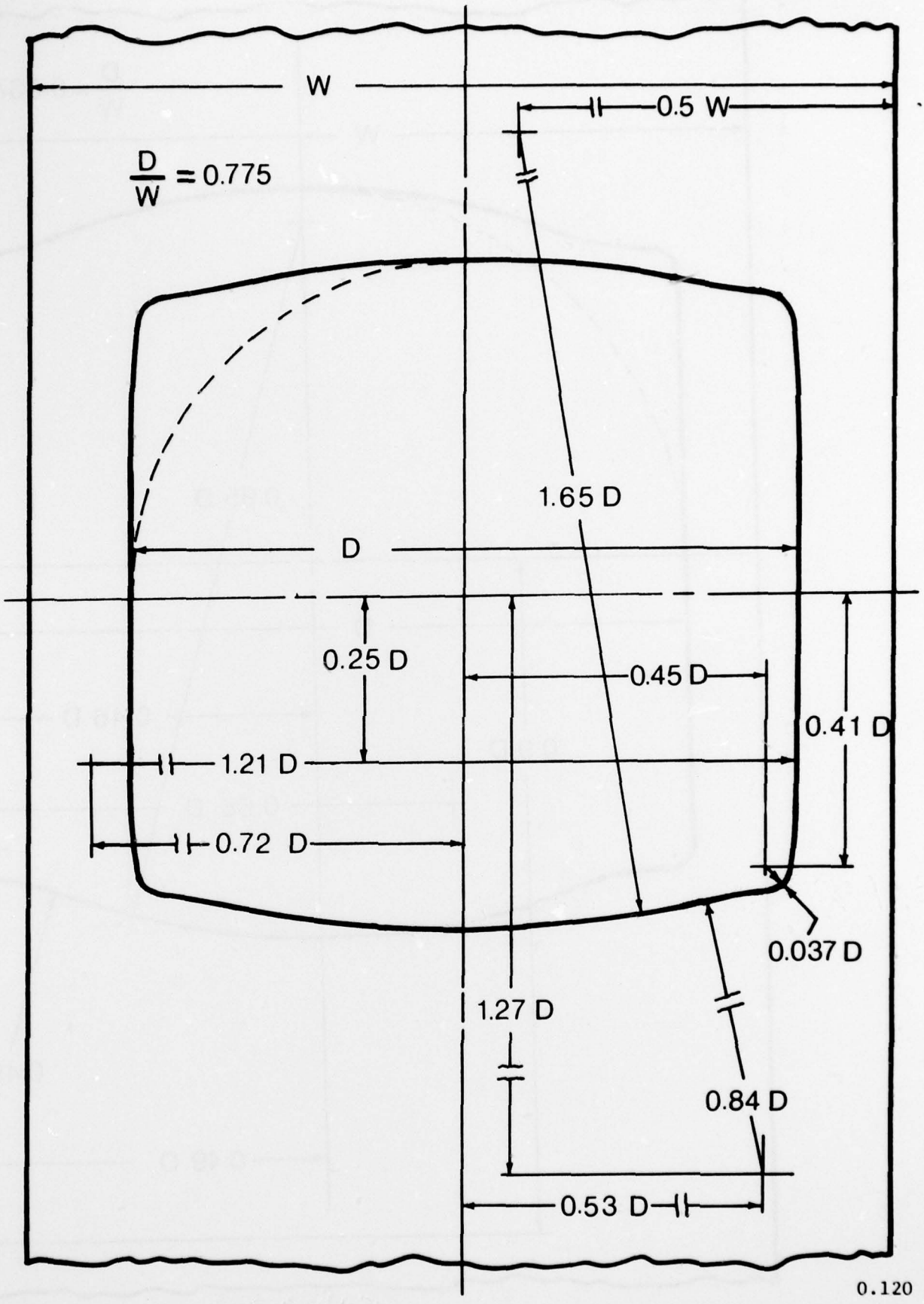

FIG. 8 OPTIMIZED GEOMETRY OF A QUASI-SQUARE HOLE IN A FINITE PLATE (D/W = 0.775) SUBJECTED TO IN-PLANE AXIAL LOADING

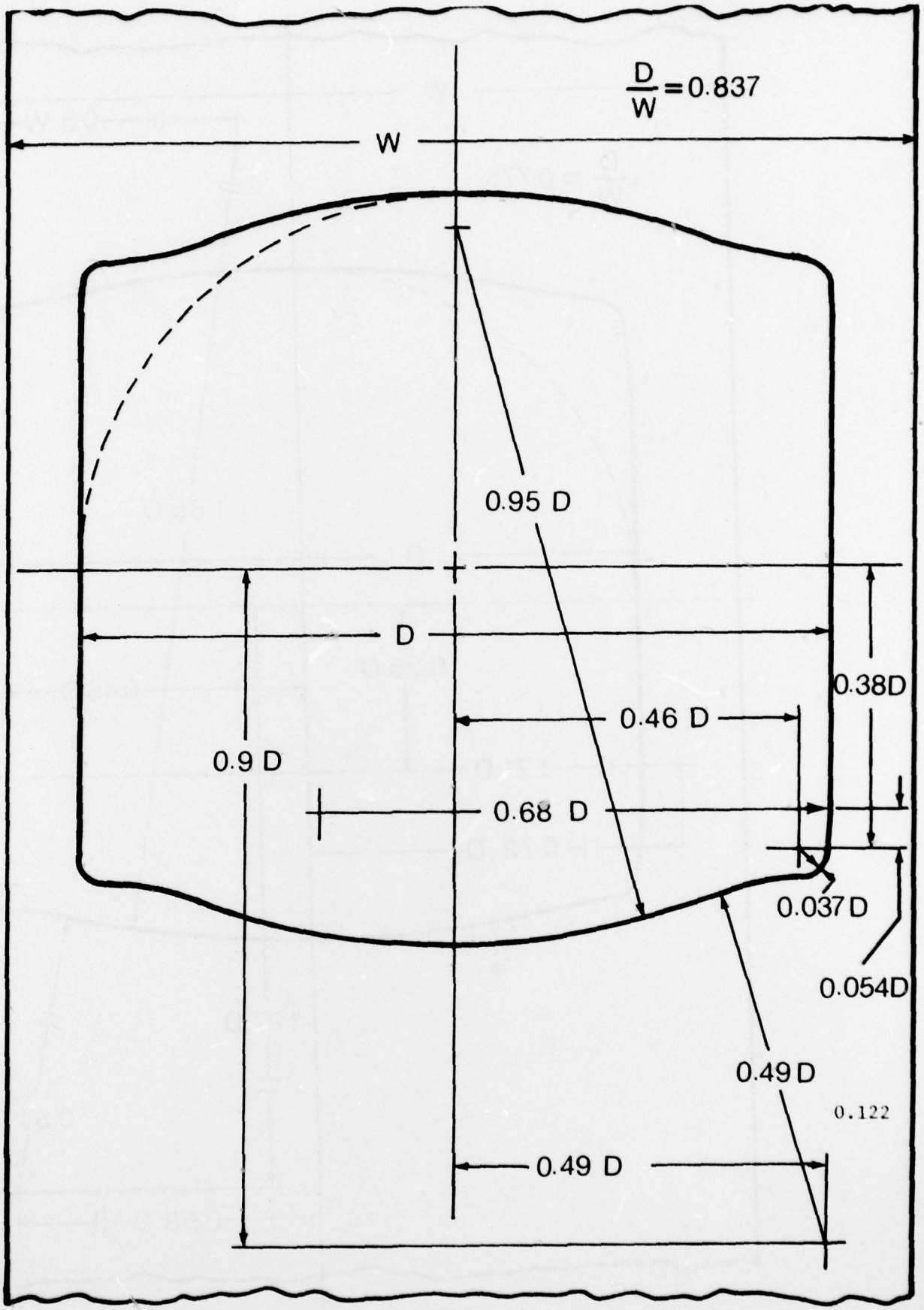

FIG. 9 OPTIMIZED GEOMETRY OF A QUASI-SQUARE HOLE IN A FINITE PLATE (D/W = 0.837) SUBJECTED TO IN-PLANE AXIAL LOADING

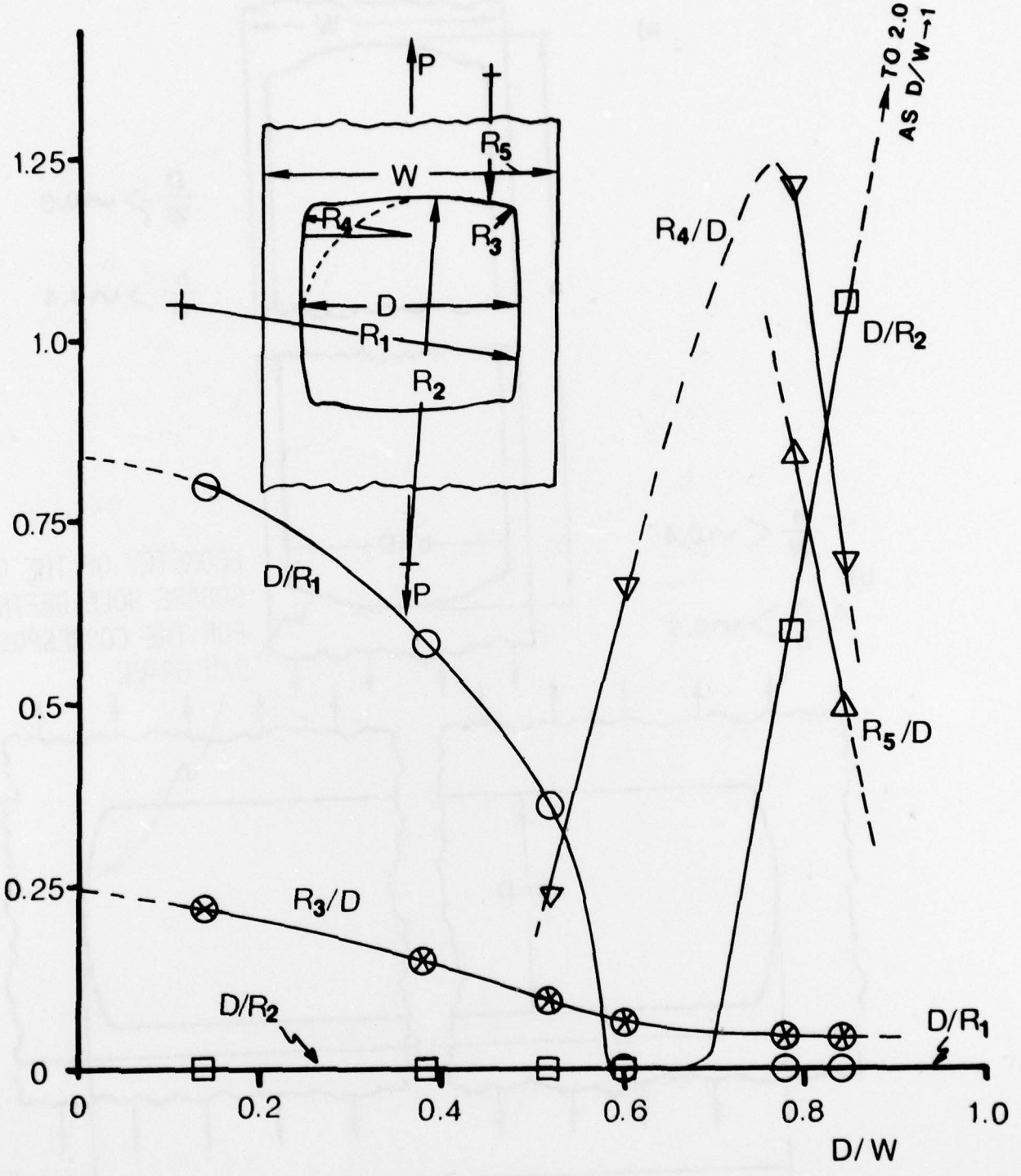

0.123

FIG. 10 RADII OF THE ELEMENTS OF THE HOLES PRODUCING OPTIMUM DISTRIBUTION OF STRESS IN FINITE PLATES, SUBJECTED TO IN-PLANE AXIAL LOADING

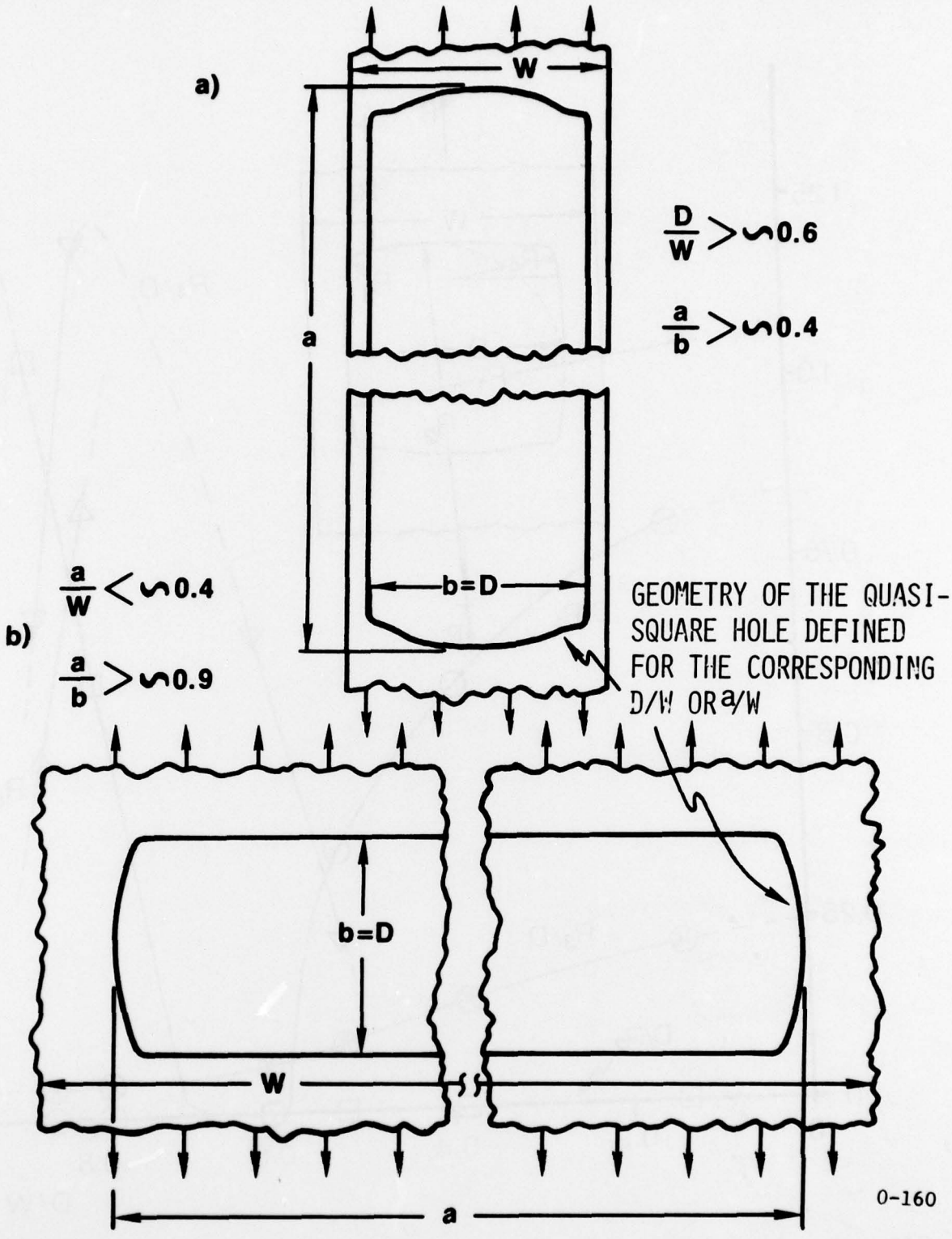

FIG. 11 OPTIMUM SHAPE FOR RECTANGULAR HOLES IN PLATES SUBJECTED TO IN-PLANE AXIAL LOADING. (GENERALIZATION OF THE QUASI-SQUARE OPTIMUM SHAPE)

ONR DISTRIBUTION LIST

Government

Office of Naval Research
Department of the Navy
Arlington, VA 22217
Attn: Code 474 (2)

Office of Naval Research
Department of the Navy
Arlington, VA 22217
Attn: Code 471 (2)

Office of Naval Research
Department of the Navy
Arlington, VA 22217
Attn: Code 200 (2)

Director
ONR Branch Office
666 Summer Street
Boston, MA 02210

Director
ONR Branch Office
536 South Clark Street
Chicago, IL 60605

Director
ONR - New York Area Office
715 Broadway - 5th Floor
New York, NY 10003

Director
ONR Branch Office
1030 East Green Street
Pasadena, CA 91106

Naval Research Laboratory (6)
Code 2627
Washington, D.C. 20375

Defense Documentation Center
Cameron Station (12)
Alexandria, VA 22314

NAVY

Undersea Explosion Res. Division
Naval Ship Research & Development Center-Att. E Palmer 177
Norfolk Naval Shipyard
Portsmouth VA 23709

Naval Research Laboratory
Washington, D.C. 20375
Attn: Code 8400

Naval Research Laboratory
Washington, D.C. 20375
Attn: Code 8410

Naval Research Laboratory
Washington, D.C. 20375
Attn: Code 8430

Naval Research Laboratory
Washington, D.C. 20375
Attn: Code 8440

Naval Research Laboratory
Washington, D.C. 20375
Attn: Code 6300

Naval Research Laboratory
Washington, D.C. 20375
Attn: Code 6390

Naval Research Laboratory
Washington, D.C. 20375
Attn: Code 6380

David W. Taylor Naval Ship
Research & Development Center
Annapolis, MD 21402
Attn: Code 2740

David W. Taylor Naval Ship
Research & Development Center
Annapolis, MD 21402
Attn: Code 28

David W. Taylor Naval Ship
Research & Development Center
Annapolis, MD 21402
Attn: Code 281

U.S. Naval Weapons Center
China Lake, CA 93555
Attn: Code 4062

U.S. Naval Weapons Center
China Lake, CA 93555
Attn: Code 4520

Commanding Officer
U.S. Naval Civil Eng. Lab.
Code L31
Port Hueneme, CA 93041

Naval Surface Weapons Center
White Oak
Silver Spring, MD 20910
Attn: Code R-10

Naval Surface Weapons Center
White Oak
Silver Spring, MD 20910
Attn: Code G-402

Naval Surface Weapons Center
White Oak
Silver Spring, MD 20910
Attn: Code K-82

Technical Director
Naval Ocean Systems Center
San Diego, CA 92152

Supervisor of Shipbuilding
U.S. Navy
Newport News, VA 23607

U.S. Navy Underwater Sound
Reference Division
Naval Research Laboratory
P.O. Box 8337
Orlando, FL 32806

Chief of Naval Operations
Department of the Navy
Washington, DC 20350
Attn: Code OP-098

Strategic Systems Project Off.
Department of the Navy
Washington, DC 20376
Attn: NSP-200

Naval Air Systems Command
Department of the Navy
Washington, DC 20361
Attn: Code 5302

Naval Air Systems Command
Department of the Navy
Washington, DC 20361
Attn: Code 604

Naval Air Systems Command
Department of the Navy
Washington, DC 20361
Attn: Code 320B

Naval Air Development Center
Director, Aerospace Mechanics
Warminster, PA 18974

U.S. Naval Academy
Engineering Department
Annapolis, MD 21402

Naval Facilities Eng. Command
200 Stovall Street
Alexandria, VA 22332
Attn: Code 03 (Res. & Devel.)

Naval Facilities Engr. Command
200 Stovall Street
Alexandria, VA 22332
Attn: Code 04B

Naval Facilities Engr. Command
200 Stovall Street
Alexandria, VA 22332
Attn: Code 045

Naval Facilities Engr. Command
200 Stovall Street
Alexandria, VA 22332
Attn: Code 14114 (Tech. Lib.)

Naval Sea Systems Command
Department of the Navy
Washington, DC 20362
Attn: Code 03 (Res. & Tech.)

Naval Sea Systems Command
Department of the Navy
Washington, DC 20632
Attn: Code 037

Naval Sea Systems Command
Department of the Navy
Washington, DC 20632
Attn: Code 035

Naval Ship Engineering Center
Department of the Navy
Washington, DC 20362
Attn: Code 6105G

Naval Ship Engineering Center
Department of the Navy
Washington, DC 20362
Attn: 6114

Naval Ship Engineering Center
Department of the Navy
Washington, DC 20362
Attn: 6120D

Naval Ship Engineering Center
Department of the Navy
Washington, DC 20362
Attn: Code 6128

Naval Ship Engineering Center
Department of the Navy
Washington, DC 20362
Attn: Code 6129

Commanding Officer & Director
David W. Taylor Naval Ship
Research & Development Center
Bethesda, MD 20084
Attn: Code 042

Commanding Officer & Director
David W. Taylor Naval Ship
Research & Development Center
Bethesda, MD 20084
Attn: Code 17

Commanding Officer & Director
David W. Taylor Naval Ship
Research & Development Center
Bethesda, MD 20084
Attn: Code 172

Commanding Officer & Director
David W. Taylor Naval Ship
Research & Development Center
Bethesda, MD 20084
Attn: Code 173

Commanding Officer & Director
David W. Taylor Naval Ship
Research & Development Center
Bethesda, MD 20084
Attn: Code 174

Commanding Office & Director
David W. Taylor Naval Ship
Research & Development Center
Bethesda, MD 20074
Attn: Code 1800

Commanding Officer & Director
David W. Taylor Naval Ship
Research & Development Center
Bethesda, MD 20084
Attn: Code 1844

Commanding Officer & Director
David W. Taylor Naval Ship
Research & Development Center
Bethesda, MD 20084
Attn: Code 1102.1

Commanding Officer & Director
David W. Taylor Naval Ship
Research & Development Center
Bethesda, MD 20084
Attn: Code 1900

Commanding Officer & Director
David W. Taylor Naval Ship
Research & Development Center
Bethesda, MD 20084
Attn: Code 1901

Commanding Officer & Director
David W. Taylor Naval Ship
Research & Development Center
Bethesda, MD 20084
Attn: Code 1945

Commanding Officer & Director
David W. Taylor Naval Ship
Research & Development Center
Bethesda, MD 20084
Attn: Code 1960

Commanding Officer & Director
David W. Taylor Naval Ship
Research & Development Center
Bethesda, MD 20084
Attn: 1962

Naval Underwater Systems Center
Newport, RI 02840
Attn: Dr. R. Trainor

Naval Surface Weapons Center
Dahlgren Laboratory
Dahlgren, VA 22448
Attn: Code G04

Naval Surface Weapons Center
Dahlgren Laboratory
Dahlgren, VA 22448
Attn: Code G20

Technical Director
Mare Island Naval Shipyard
Vallejo, CA 94592

U.S. Naval Postgraduate School
Library
Code 0384
Monterey, CA 93940

Webb Institute of Naval
Architecture- Attn: Librarian
Crescent Beach Road, Glen Cove
Long Island, NY 11542

Commanding Officer (2)
U.S. Army Research Office
P.O. Box 12211
Research Triangle PK. NC 27709
Attn: J. J. Murray, CRD-AA-IP

Watervliet Arsenal
MAGGS Research Center
Watervliet, NY 12189
Attn: Director of Research

U.S. Army Materials and
Mechanics Research Center
Watertown, MA 02172
Attn: Dr. R. Shea DRXMR-T

U.S. Army Missile Research and
Development Center
Redstone Scientific Info. Cen.
Chief, Document Section
Redston Arsenal, AL 35809

Army Research & Development
Center
Fort Belvoir, VA 22060

NASA
Structures Research Division
Langley Research Center
Langley Station
Hampton, VA 23365

NASA
Associate Adm. for Advanced
Research & Technology
Washington, DC 20546

Scientific & Tech. Info. Fac.
NASA Representative (S-AK/DL)
P.O. Box 5700
Bethesda, MD 20014

Commander WADD
Wright Patterson AFB
Attn: Code WWRMDD
Dayton, OH 45433

Commander WADD
Wright Patterson AFB
Attn: Code AFFDL(FDDS)
Dayton, Oh 45433

Commander WADD
Wright Patterson AFB
Attn: Structures Div.
Dayton, OH 45433

Commander WADD
Wright Patterson AFB
Attn: Code AFLC (MCEEA)
Dayton, OH 45433

Chief Appl.Mechanics Group
U.S. Air Force Inst. of Tech.
Wright-Patterson AFB
Dayton, OH 45433

Chief, Civil Engr. Branch
WLRC, Research Division
Air Force Weapons Laboratory
Kirtland AFB, Albuquerque, NM
87117

Air Force Office of Scientific
Research
Bolling Air Force Base
Washington, DC 20332
Attn: Mechanics Div.

Department of the Air Force
Air University Library
Maxwell Air Force Base
Montgomery, AL 36112

Commandant
Chief, Testing & Devel. Div.
U.S. Coast Guard
1300 E Street, NW
Washington, D.C 20226

Technical Director
Marine Corps Devl. & Educ.
Command
Quantico, VA 22134

Director Defense Research & Egr.
Technical Lib. Rm 3C-128
The Pentagon
Washington, D.C. 20301

Director
National Bureau of Standards
Washington, DC 20034
Attn: B. L. Wilson, EM 219

Dr. M. Gaus
National Science Foundation
Environmental REsearch Div.
Washington, DC 20550

Library of Congress
Science & Technology Div.
Washington, DC 20540

Director
Defense Nuclear Agency
Washington, DC 20305
Attn: SPSS

Mr. Jerome Persh
Staff Specialist for Materials
and Structures
OUSDR&E, The Pentagon-Rm 3D1089
Washington, DC 20301

Chief, Airframe & Equipment
Branch - FS-120
Office of Flight Standards
Federal Aviation Agency
Washington, DC 20553

National Academy of Sciences
National Research Council
Ship Hull Research Committee
2101 Constitution Avenue
Washington, DC 20418(A.R.Lytle)

National Science Foundation
Engineering Mechanics Section
Division of Engineering
Washington, DC 20550

Picatinny Arsenal
Plastics Tech. Evaluation Center
Attn: Technical Info. Section
Dover, NJ 07801

Maritime Administration
Office of Maritime Technology
14th & Constitution Ave., NW
Washington, DC 20230

Maritime Administration
Office of Ship Construction
14th & Constitution AVE., NW
Washington, DC 20230

Dr. H. H. Vanderveldt
Dept. of the Navy
Naval Sea Systems-Code 03522
Washington, D.C. 20362

UNIVERSITIES

Dr. J. Tinsley Oden
University of Texas at Austin
345 Engr. Science Building
Austin, TX 78712

Professor Walter D. Pilkey
University of Virginia
Res. Lab. for Egr. Sciences
School of Egr. & Appl. Sciences
Charlottesville, VA 22901

Professor Albert I. King
Wayne State University
Biomechanics Research Center
Detroit, MI 48202

Prof. Julius Miklowitz
California Inst. of Technology
Div. of Engr. & Appl Science
Pasadena, CA 91109

Professor K. D. Willmert
Clarkson College of Technology
Dept. of Mechanical Engineering
Potsdam, NY 13676

Dr. V. R. Hodgson
Wayne State University
School of Medicine
Detroit, MI 48202

Dr. Harold Liebowitz, Dean
School of Engr. & Appl. Science
George Washington University
Washington, DC 20052

Dr. Walter E. Haisler
Texas A&M University
Aerospace Engineering Department
College Station, TX 77843

Dean B. A. Boley
Northwestern University
Department of Civil Engineering
Evanston, IL 60201

Professor Eli Sternberg
California Inst. of Technology
Div. of Engr. & Appl. Science
Pasadena, CA 91109

Dr. Hussein A. Kamel
University of Arizona
Dept. of Aero. & Mechanical Egr.
Tucson, AZ 85721

Professor P. G. Hodge, Jr.
University of Minnesota
Dept. of Aero. Egr. & Mech.
Minneapolis, MN 55455

Professor Paul M. Naghdi
University of California
Dept. of Mechanical Engr.
Berkeley, CA 94720

Dr. S. J. Fenves
Carnegie-Mellon University
Dept. of Civil Engineering
Schenley Park
Pittsburgh, PA 15213

Dr. D. C. Drucker
University of Illinois
Dean of Engineering
Urbana, IL 61801

Professor F. L. DiMaggio
Columbia University
Dept. of Civil Engineering
New York, NY 10027

Dr. Ronald L. Huston
Dept. of Engineering Analysis
University of Cincinnati
Cincinnati, OH 45221

Professor N. M. Newmark
University of Illinois
Department of Civil Engineering
Urbana, IL 61803

Professor Norman Jones
MIT
Dept. of Ocean Engineering
Cambridge, MA 02139

Prof. G. C. M. Sih
Lehigh University
Inst. of Fracture & Solid Mech.
Bethlehem, PA 18015

Professor E. Reissner
Univ. of California, San Diego
Dept. of Applied Mechanics
La Jolla, CA 92037

Prof. E. J. Skudrzyk
Pennsylvania State University
Applied Research Laboratory
Department of Physics
State College, PA 16801

Prof. Albert S. Kobayashi
University of Washington
Dept. of Mechanical Engineering
Seattle, WA 98105

Professor William A. Nash
University of Massachusetts
Dept. of Mech. & Aero. Egr.
Amherst, MA 01002

Professor J. Kempner
Polytechnic Inst. of New York
Dept. of Aero.Egr.,Appl.Mech
333 Jay Street
Brooklyn, NY 11201

Professor Daniel Frederick
Virginia Polytechnic Inst. &
State University
Dept. of Engineering Mechanics
Blacksburg, VA 24061

Professor G. Herrmann
Stanford University
Dept. of Applied Mechanics
Stanford, CA 94305

Professor J. Klosner
Polytechnic Inst. of New York
Dept. of Aero.EGR., Appl.Mech.
333 Jay Street
Brooklyn, NY 11201

Professor A. C. Eringen
Princeton University
Dept. of Aero. & Mechanical Sci.
Princeton, NJ 08540

Professor J. D. Achenbach
Northwestern University
Dept. of Civil Engineering
Evanston, IL 60201

Professor R. A. Schapery
Texas A&M University
Dept. of Civil Engineering
College Station, TX 77843

Professor E. H. Lee
Stanford University
Div. of Engineering Mechanics
Stanford, CA 94305

Professor S. B. Dong
University of California
Dept. of Mechanics
Los Angeles, CA 90024

Professor Burt Paul
University of Pennsylvania
Towne School of Civil and
Mechanical Engineering
Philadelphia, PA 19104

Dr. Samuel B. Batdorf
University of California
School of Engr.&Appl. Science
Los Angeles, CA 90024

Professor Charles W. Bert
University of Oklahoma
School of Aerospace., Mechanical
and Nuclear Engineering
Norman, OK 73019

Professor H. W. Liu
Syracuse University
Dept. of Chemical EGR & Metal.
Syracuse, NY 13210

Professor Michael Pappas
New Jersey Inst. of Technology
Newark College of Engineering
323 High Street
Newark, NJ 07102

Professor Satya N. Atluri
Georgia Inst. of Technology
School of Egr. Sci & Mech.
Atlanta, GA 30332

Professor S. Bodner
Technion R & D Foundation
Haifa, Israel

Professor E. Krempl
Rensselaer Polytechnic Inst.
Division of Engineering
Engineering Mechanics
Troy, NY 12181

Professor Graham F. Carey
University of Texas at Austin
Dept. of Aero. Egr. & Egr.Mech.
Austin, TX 78712

Professor Werner Goldsmith
University of California
Department of Mech. Engr.
Berkeley, CA 94720

Dr. Jack R. Vinson
University of Delaware
Dept. of Mech & Aero. Engr.
and Center for Composite Matls.
Newark, DL 19711

Dr. Jackson C. S. Yang
Advanced Tech. & Research, Inc.
10006 Green Forest Drive
Adelphi, MD 20783

Professor R. S. Rivilin
Lehigh University
Center for Appl. of Math.
Bethlehem, PA 18015

Dr. Dennis A. Nagy
Princeton University.
School of Engr. & Appl. Science
Dept. of Civil Engineering
Princeton, NJ 08540

Dr. Norman Hobbs
Kaman AviDyne
Division of Kaman Sci. Corp.
Burlington, MA 01803

Professor F. A. Cozzarelli
SUNY at Buffalo
Div. of Inter. Studies
Karr Parker Egr. Bldg.
Buffalo, NY 14214

Dr. J. Duffy
Brown University
Division of Engineering
Providence, RI 02912

Argonne National Laboratory
Library Services Department
9700 South Cass Avenue
Argonne, IL 60440

Professor Joseph L. Rose
Drexel University
Dept. of Mech. Egr. & Mech.
Philadelphia, PA 19104

Dr. J. L. Swedlow
Carnegie-Mellon University
Dept. of Mechanical Engineering
Pittsburgh, PA 15213

Dr. M. C. Junger
Cambridge Acoustical Assoc.
1033 Massachusetts Avenue
Cambridge, MA 02138

Professor B. K. Donaldson
University of Maryland
Aerospace Engineering Dept.
College Park, MD 20742

Dr. V. K. Varadan
Ohio State Un. Res. Foundation
Dept. of Engineering Mechanics
Columbus, OH 43210

Dr. V. Godino
General Dynamics Corporation
Electric Boat Division
Groton, CT 06340

Professor Joseph V. Clark
Catholic University of America
Dept. of Mechanical Engr.
Washington, DC 20064

Dr. Jackson C. S. Yang
University of Maryland
Dept. of Mechanical Engineering
College Park, MD 20742

Dr. J. E. Greenspon
J.G. Engineering Research Assoc.
3831 Menlo Drive
Baltimore, MD 21215

Professor T. C. Huang
University of Wisc.-Madison
Dept. of Eng. Mechanics
Madison, WI 53706

Dr. Z. Hashin
University of Pennsylvania
Dept. of Metallurgy & Mats. Sci.
College Of Engr. & Appl. Sci
Philadelphia, PA 19104

Dr. K. C. Park
Lockheed Missile & Space Co.
3251 Hanover Street
Palo Alto, CA 94304

Professor Isaac Fried
Boston University
Dept. of Mathematics
Boston, MA 02215

Dr. T. Y. Chang
University of Akron
Department of Civil Engineering
Akron, OH 44325

Newport News Shipbuilding and
Dry Dock Company
Library
Newport News, VA 23607

Dr. M. F. Bozich
McDonnell Douglas Corp.
5301 Bolsa Avenue
Huntington Beach, CA 92647

Dr. H. N. Abramson
Southwest Research Institute
8500 Culebra Road
San Antonio, TX 78284

Dr. R. C. DeHart
Southwest Research Institute
8500 Culebra Road
San Antonio, TX 78284

Dr. M. L. Baron
Wiedlinger Associates
110 East 59th Street
New York, NY 10022

Dr. T. L. Geers
Lockheed Missiles & Space Co.
3251 Hanover Street
Palo Alto, CA 94304

Mr. William Caywood
Applied Physics Laboratory
Johns Hopkins Road
Laurel, MD 20810

Dr. Robert E. Nickell
Pacifica Technology
P.O. Box 148
Del Mar, CA 92014

Dr. M. F. Kanninen
Battelle Columbus Labs.
505 King Avenue
Columbus, OH 43201

Dr. G. T. Hahn
Battelle Columbus Labs.
505 King Avenue
Columbus, OH 43201

Dr. A. A. Hochrein
Daedalean Associates, Inc.
Springlake Research Center
15110 Frederick Road
Woodbine, MD 21797

Mr. Richard Y. Dow
National Academy of Sciences
2101 Constitution Avenue
Washington, DC 20418

Mr. H. L. Kington
Airesearch Mfg. Co. of Arizona
P.O. Box 5217
111 South 34th Street
Phoenix, AZ 85010

Dr. M. H. Rice
Systems, Science & Software
P.O. Box 1620
La Jolla, CA 92037

SECURITY CLASSIFICATION OF THIS PAGE (When Data Entered)

REPORT DOCUMENTATION PAGE

READ INSTRUCTIONS BEFORE COMPLETING FORM

1. REPORT NUMBER: (14) 50
2. GOVT ACCESSION NO.
3. RECIPIENT'S CATALOG NUMBER

4. TITLE (and Subtitle): (6) OPTIMUM HOLE SHAPES IN FINITE PLATES UNDER UNIAXIAL LOAD
5. TYPE OF REPORT & PERIOD COVERED
6. PERFORMING ORG. REPORT NUMBER

7. AUTHOR(s): (10) A. J. Durelli [redacted] K. Rajaiah
8. CONTRACT OR GRANT NUMBER(s): (15) N00014-76-C-0487, NSF-ENG77-07974

9. PERFORMING ORGANIZATION NAME AND ADDRESS
Oakland University
Rochester, MI 48063

10. PROGRAM ELEMENT, PROJECT, TASK AREA & WORK UNIT NUMBERS

11. CONTROLLING OFFICE NAME AND ADDRESS
Office of Naval Research
Department of the Navy
Washington, D. C. 20025

12. REPORT DATE: Feb[redacted]1979
13. NUMBER OF PAGES: 34

14. MONITORING AGENCY NAME & ADDRESS (if different from Controlling Office): (12) 38p.
15. SECURITY CLASS. (of this report): Unclassified
15a. DECLASSIFICATION/DOWNGRADING SCHEDULE

16. DISTRIBUTION STATEMENT (of this Report)
Distribution of this report is unlimited

17. DISTRIBUTION STATEMENT (of the abstract entered in Block 20, if different from Report)

18. SUPPLEMENTARY NOTES

19. KEY WORDS (Continue on reverse side if necessary and identify by block number)

Optimization	Photoelasticity
Quasi-Square Hole	Square Hole
Stress Concentration	Finite Plate

20. ABSTRACT (Continue on reverse side if necessary and identify by block number)

This paper presents optimized hole shapes in plates of finite width subjected to uniaxial load for a large range of hole to plate widths (D/W) ratios. The stress concentration factor for the optimized holes decreased by as much as 44% when compared to circular holes. Simultaneously, the area covered by the optimized hole increased by as much as 26% compared to the circular hole. Coefficients of efficiency between 0.91 and 0.96 are achieved. The geometries of the optimized holes for

DD FORM 1 JAN 73 1473 EDITION OF 1 NOV 65 IS OBSOLETE
S/N 0102-014-6601 |

SECURITY CLASSIFICATION OF THIS PAGE (When Data Entered)

405 252

the D/W ratios considered are presented in a form suitable for use by designers. It is also suggested that the developed geometries may be applicable to cases of rectangular holes and to the tip of a crack. This information may be of interest in fracture mechanics.